Analysis of Novel Sensors and Satellite Formation Flights for Future Gravimetry Missions

Alexey Kupriyanov, Arthur Reis, Annike Knabe, Nina Fletling, Alireza HosseiniArani, Mohsen Romeshkani, Manuel Schilling, Vitali Müller, and Jürgen Müller

Abstract

Accelerometers (ACCs) in low-low satellite-to-satellite gravimetry missions measure the non-gravitational forces acting on the spacecraft that have to be taken into account to derive the gravitational contribution in the distance variations. Multiple ACCs form a so-called gradiometer that measure the gravity gradient. In satellite gravimetry up to now, only electrostatic ACCs were used, which are one of the main instrumental limitations due to their error contribution at low frequencies, known as drift.

In this paper, we compare the performance of electrostatic ACCs at low Earth orbits with other sensors, i.e. so-called Optical ACCs based on flight heritage of the LISA-Pathfinder mission, and theoretical ACC concepts, for example Cold Atom Interferometer (CAI) ACCs and hybridized sensors (combination of electrostatic and CAI ACCs) in terms of static gravity field recovery. Under our assumptions, in particular that high-frequency variations of the gravity field can be perfectly modeled and removed during gravity field recovery, the results may be limited in the future by the performance of the LRI.

We also discuss the outcomes from the various novel satellite formation flights (SFF) that utilize two orbits that differ either by right ascension of the ascending node (RAAN) or by inclination in order to acquire ranging information in the cross-track direction. The closed-loop simulations from both scenarios showed significantly lower order of magnitude of the residuals w.r.t. reference gravity field than from the anticipated future performance of the solely in-line GRACE-like satellite pair. Moreover, these triple satellite formations provide better multi-directionality of the retrieved data, avoiding the North-South striping behavior. However, it is worth noting that in such formations significant modifications are needed in the satellite bus, ACC test mass readout, LRI beam steering mechanism, etc. in order to be capable of measuring the cross-track range changes at higher range rates w.r.t.

A. Kupriyanov (✉) · A. Knabe · N. Fletling · A. HosseiniArani · M. Romeshkani · J. Müller
Institute of Geodesy, Leibniz University Hannover, Hannover, Lower Saxony, Germany
e-mail: kupriyanov@ife.uni-hannover.de; knabe@ife.uni-hannover.de; fletling@ife.uni-hannover.de; hosseiniarani@ife.uni-hannover.de; romeshkani@ife.uni-hannover.de; mueller@ife.uni-hannover.de

A. Reis · V. Müller
Max Planck Institute for Gravitational Physics (IGP), Albert Einstein Institute, Hannover, Lower Saxony, Germany

Institute for Gravitational Physics, Leibniz University Hannover, Hannover, Lower Saxony, Germany
e-mail: arthur.reis@aei.mpg.de; vitali.mueller@aei.mpg.de

M. Schilling
Institute for Satellite Geodesy and Inertial Sensing, German Aerospace Center (DLR), Hannover, Lower Saxony, Germany
e-mail: manuel.schilling@dlr.de

in-line GRACE-like configuration. In addition, a substantial reduction of costs in building and launching only three satellites rather than four as in double-pair constellations could be an advantage for such formations.

1 Introduction

Dedicated satellite gravimetry missions such as CHAMP (Mehta et al. 2017; Torge et al. 2023), GOCE (Flechtner et al. 2021), GRACE (Chen et al. 2022; Panet et al. 2022), its successor GRACE-FO (Peidou et al. 2022) and a Chinese satellite gravimetry pair (Xiao et al. 2023) provide unique data about Earth's gravity field variations at different spatio-temporal scales. However, despite the impressive results from the above-mentioned missions with unprecedented accuracy at the time when they were obtained, there was a common limiting factor on the instrument level. This well-known limitation results from the behaviour of the electrostatic accelerometer (EA), which shows a so-called drift in the low frequency domain (Frommknecht et al. 2003; van Camp et al. 2021), mainly caused by the polarization wire that connects the test mass to the surrounding electrode housing and is a significant source of stiffness (Christophe et al. 2015).

In order to overcome the drawback of EAs and better satisfy the user needs discussed by Pail et al. (2015), various concepts and novel technologies were developed. For example, enhanced EAs with modified test mass parameters were analyzed by the French aerospace lab ONERA (Liorzou et al. 2023). Another technical improvement that has been preliminary evaluated by ONERA (Boulanger et al. 2020) is the use of an EA without a polarization wire. It was substituted by a wireless charge management system utilizing ultraviolet light, which excites and expels extra electrons and keeps the electrostatic noise sources at low frequencies at an acceptable level (Sumner et al. 2020). This technology has flight heritage since it was on-board the LISA-Pathfinder mission (Armano et al. 2021) where optical accelerometers, also known as Gravitational Reference Sensor (GRS), were also tested in space for the first time (Armano et al. 2018). Promising results of the GRS from the LISA-Pathfinder gave a start to various studies that evaluate the performance of a simplified-GRS (SGRS) for low Earth orbits. SGRS is an enhanced EA with a free-floating cubic shaped test mass, with capacitive position readout sensing and without polarization wire proposed by Dávila Álvarez et al. (2022) and LISA-like SGRS by Weber et al. (2022). SGRS with a

wider range of parameters, electrostatic and optical readouts of the test mass displacements was modeled and evaluated by Kupriyanov et al. (2024).

A totally different technology that could overcome the drawback of EAs at low frequencies is the Cold Atom Interferometry (CAI) where atom clouds act as test masses (Alonso et al. 2022). In CAI accelerometry, the unknown acceleration is calculated from the phase shift of two interfering atomic states of an atom cloud after it was manipulated with pulses of two counter propagating laser beams. Corresponding studies evaluating CAI accelerometry were done by Knabe et al. (2022) and for the usage in gradiometry by Trimeche et al. (2019). However, the utilization of a CAI accelerometer as a standalone instrument has certain drawbacks due to the long interrogation times in which affected short-term non-gravitational forces could not be observed. A possibility to solve this problem is the application of hybridization. Here, the idea is to combine the EA, which are able to measure in the high frequency domain, with the precise CAI ACC. HosseiniArani et al. (2022) and Zahzam et al. (2022) studied hybrid sensors and different ways of hybridization.

It is important to note, that in contrast to EA or optical accelerometers, CAI has not yet a flight heritage in space. However, the recently started CARIOQA-PMP (Cold Atom Rubidium Interferometer in Orbit for Quantum Accelerometry – Pathfinder Mission Preparation) project, funded by the European Union, aims to increase the Technology Readiness Level and prepare a Quantum Pathfinder Mission for space gravimetry by 2030 (Lévèque et al. 2023).

2 Performance of Sensors

2.1 Comparison of Accelerometer Performance

In Fig. 1 the Amplitude Spectral Density (ASD) of various ACCs types are shown w.r.t. typical non-gravitational accelerations (black curve). The above-mentioned drift of the EA that is used in GRACE-FO (Daras and Pail 2017) (grey curve) is very prominent in the frequencies below 1 mHz. Another EA which was used in GOCE mission has a similar
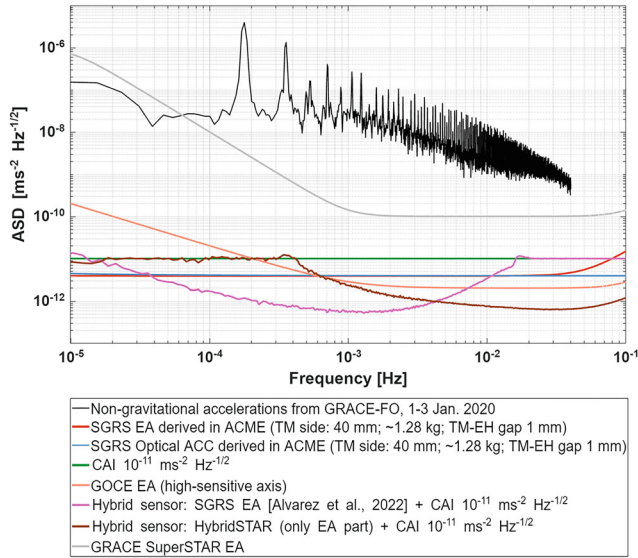
Fig. 1 Comparison of the ASD sensitivities of accelerometers for current instruments and anticipated enhanced concepts w.r.t. non-gravitational accelerations measured by GRACE-FO

Fig. 2 Comparison of the ASDs of the inter-satellite LRI and KBR range measurement instrument errors used in the studies

2.2 Comparison of Inter-Satellite Range Measurement Instruments

Figure 2 shows the ASDs of the inter-satellite LRI and K-band ranging (KBR) measurement instrument errors. The grey curve corresponds to the KBR instrument that is used in GRACE and GRACE-FO (Frommknecht et al. 2006). All other curves represent our assumptions on the distance-dependent errors of Laser Range Interferometer (LRI) system on-board GRACE-FO (green curve) or the anticipated LRI error noise in the future (red and blue curves) (Kupriyanov et al. 2024).

drift. The orange curve represents the high-sensitive axis of the accelerometer that forms the gradiometer (Touboul et al. 2016; Marque et al. 2010). The red and blue curves represent the noise levels of SGRS sensors with electrostatic and optical test mass position readout, developed by Kupriyanov et al. (2024). Due to the modeling features of the noise budgets of these SGRS sensors, the difference of their ASDs appears only above 0.01 Hz. The green curve represents the realistic level of accuracy in one degree of freedom of a near-future CAI ACC introduced by white noise at the level of $10^{-11}\,\mathrm{m/s^2}/\sqrt{\mathrm{Hz}}$. For this sensor the following major parameters were assumed: laser waist 20×10^{-3}m, atomic temperature 10×10^{-12}K, number of atoms 1×10^6, interrogation time 10 s (HosseiniArani et al. 2024). As it was demonstrated by Barrett et al. (2019), achieving a same level of accuracy in all three axes for CAI inertial sensor is quite challenging. Additionally, two curves of hybrid sensors are shown in the same graph. The pink curve corresponds to a hybridized instrument that consists of an SGRS EA from Dávila Álvarez et al. (2022) and the aforementioned CAI ACC. The hybridization was done at the level of ASDs by applying low- and high-pass filters at two cut-off frequencies at 11 mHz and 17 mHz in order to have a smooth transition between the ASDs. A similar procedure was applied for the hybridization of another sensor (brown curve) that consists of an electrostatic part of the HybridSTAR accelerometer (Dalin et al. 2020) and the CAI ACC. Here, only one cut-off frequency at 0.35 mHz was used for both low- and high-pass filters.
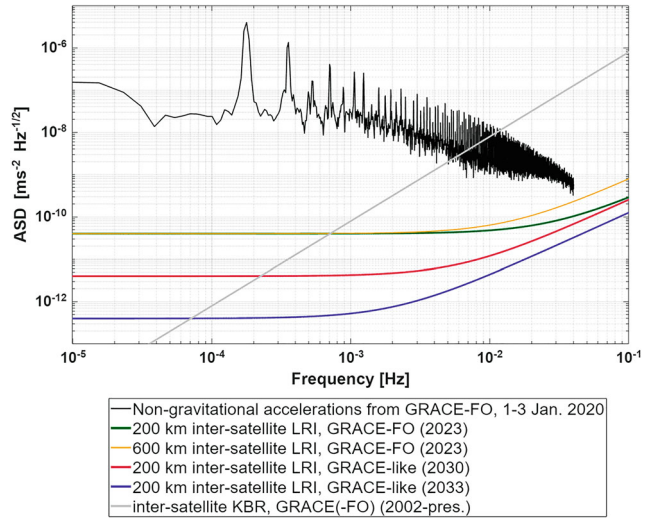
3 Closed-Loop Simulation

The block diagram of the closed-loop simulation procedure that was applied in the context of GRACE-like, GOCE-like and novel satellite constellations is shown in Fig. 3. The simulation procedure was carried out in multiple steps and using software parts in different language tools and programming platforms. In all simulations the EIGEN-6C4 (Förste et al. 2011) static gravity field model was used as the reference. The time-variable background models were not considered in our simulations in order to focus on the advantages of the novel sensors and concepts. Therefore, this study investigates the retrieval of the static gravity field. The evaluation is carried out on the level of residuals between recovered and reference gravity field models that occur due to considering various error sources, i.e. instrument errors.
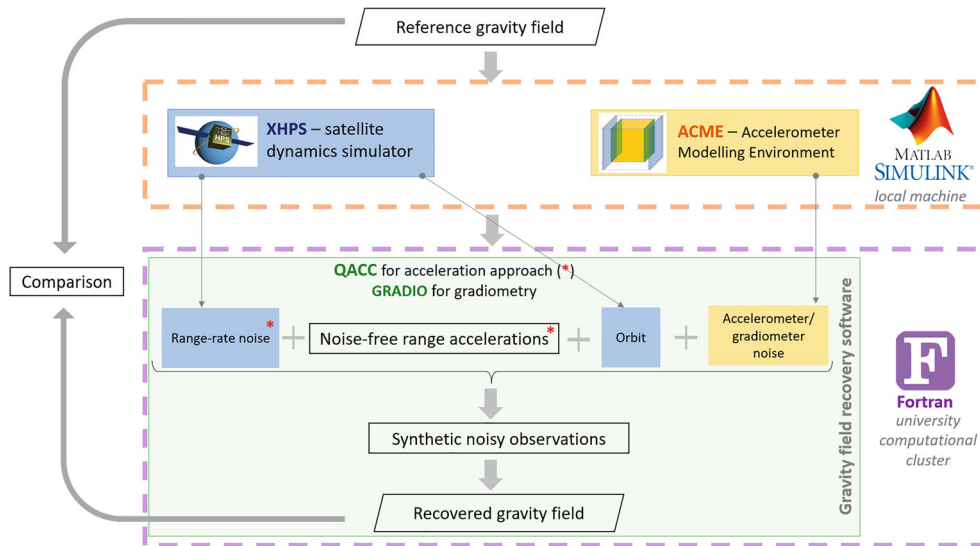
Fig. 3 Block diagram of the closed-loop simulation procedure

The Extended High Performance Satellite Dynamics Simulator (XHPS) developed by ZARM/DLR (Wöske et al. 2016) in Matlab/Simulink is used for simulating the satellite's orbit taking into account various non-gravitational forces and a detailed finite element model of the satellite (Wöske et al. 2018). Accelerometer Modeling Environment (ACME) (Kupriyanov et al. 2024) developed by Max Planck Institute for Gravitational Physics is also implemented in Matlab/Simulink and utilize to simulate different type of ACCs, e.g. electrostatic or optical ones. In this work ACME is operated concurrent to XHPS, running time-domain simulations and generating mock data of various sensors. Two gravity field recovery software tools, named Quantum Accelerometry (QACC) and GRADIO, both developed by IfE, LUH (Wu 2016) written in Fortran are used in the simulations.

For the GRACE-like cases QACC toolbox with acceleration approach is used. Here the noise-free range accelerations time-series are generated and combined afterwards with corresponding instrument noise time-series, i.e. range-rate sensor noise, LRI or KBR (Frommknecht et al. 2006) and with ACC noise. Then the synthesized noisy observations are used for least-squares estimation of the gravity field parameters – spherical harmonic coefficients. At the end the recovered gravity field is compared with the reference gravity field, by computing the difference of the coefficients and plotting them either on a global map in terms of equivalent water height (EWH) or in two dimensional spherical harmonic error spectrum (similar as it was done by Wu (2016)).

For the gravity field recovery from the GOCE-like gradiometry missions GRADIO toolbox is used. There, the satellites' orbit from XHPS synthesised together with the corresponding gradiometer noise time-series. Then following the aforementioned steps the retrieved gravity field are compared with the reference one.

4 Gravity Field Recovery Results from Simulation

For all simulations a one-month mission duration in May 2002 was considered, since this was a period of strong solar activity (SILSO World Data Center 2023). As a result, high solar activity means that the solar radiation pressure and the air-drag on the spacecraft in orbit are larger. The selection of the year/month with the high solar activity was important for the testing accelerometers, developed in ACME, in critical conditions. Furthermore, all gravity field recovery simulations were calculated up to degree and order 180, while the input reference gravity field model was given up to degree and order 2190.

4.1 Low-Low Satellite-to-Satellite

Figure 4 represents the averaged error degree variance per specific degree in terms of geoid height for the low-low satellite-to-satellite (ll-sst) missions on a GRACE-like orbit with different types of ACCs and inter-satellite range instruments. Black dashed line represent the static gravity field signal EIGEN-6C4 (Förste et al. 2011). The mean monthly Hydrology, Ice and solid Earth (HIS) signal (Dobslaw et al. 2015), depicted by the grey dashed curve. This curve is shown here for the understanding that in an idealized case, when the temporal aliasing is sufficiently considered and the high performance of the instruments can be fully exploited,
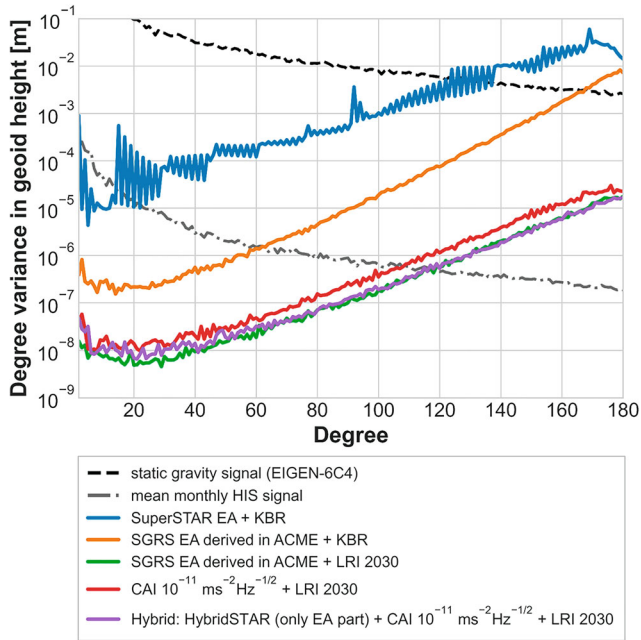
Fig. 4 Averaged error degree variance per specific degree in terms of geoid height of the different on-board ACC and inter-satellite range instruments in the context of GRACE-FO like missions

potentially time-variable gravity field can be determined up to a much higher degree and order than now. The blue curve represents the GRACE-FO mission with a SuperSTAR EA and KBR as the range measurement instrument. The static gravity field signal could be resolved up to degree 130 by this mission and the mean monthly HIS signal only up to degree 15. The strong oscillations of the blue curve corresponds to the drift of the EA in the low frequency domain. The orange and green curves represent the missions with a SGRS EA, derived in ACME, on-board and KBR or an anticipated LRI of the year 2030 as the inter-satellite instrument. In comparison to the GRACE-FO scenario with a maximum achievable level of a geoid height 10^{-5} m, these mission concepts are able to reach 10^{-7} m and 10^{-8} m respectively. They also can potentially resolve the time-variable HIS signal under the above-mentioned conditions up to degree 60 and 120. The CAI ACC as a standalone accelerometer together with the anticipated LRI 2030 performance (red curve) shows a slightly worse performance w.r.t. the previously discussed SGRS EA with LRI 2030. Hybridizing a CAI ACC with an electrostatic part of the HybridSTAR accelerometer together with the LRI 2030 (purple curve) brings only minor improvements w.r.t. the standalone CAI ACC case (red curve). However, the SGRS EA derived in ACME with LRI 2030 (green curve) shows the best performance up to degree 60 among the considered sensors.

4.2 Cross-Track Gradiometry

Since the ll-sst type of measurements and satellite gradiometry are both sensitive to different wavelengths of the gravity field signal (Pail et al. 2019), we also checked the performance of novel instruments w.r.t. high-sensitive axis of the GOCE electrostatic gradiometer (Touboul et al. 2016; Marque et al. 2010) arranged in the cross-track direction. Gradiometry simulations were computed for the GOCE-like altitude, near-polar, drag-compensated orbit ($i = 89°$, $h = 246$ km) with a gradiometer arranged in cross-track direction with a baseline length $b = 0.5$ m.

Figure 5 shows the average error degree variance per specific degree for various gradiometer instruments. The blue curve corresponds to the GOCE high-sensitive axis of the electrostatic gradiometer, acquired from the ASD orange curve from Fig. 1. The orange and green curves in Fig. 5 correspond to the gradiometers that consist of SGRS EA or an optical ACC. Simulated CAI and hybridized gradiometers also include the effect of CAI gyroscopes (Savoie et al. 2018) which are required to correct for the rotational movement of the gradiometer axis in cross-track direction. The considered CAI gyroscope has a white-noise level close to 10^{-8} rads^{-1} in terms of angular velocity which corresponds to interrogation time of 10 s. However, the effect of the
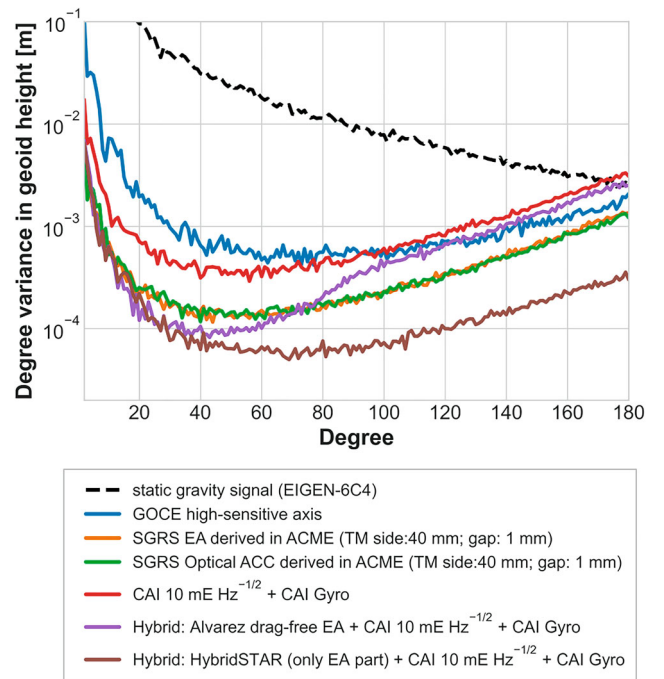

Fig. 5 Averaged error degree variance per specific degree in terms of geoid height of the different gradiometers in cross-track direction in the context of a potential GOCE-FO like mission

CAI gyroscope to the total CAI or hybridized gradiometer performance was negligibly small. As it is depicted in the graph, hybridized gradiometers show the best performance roughly up to degree 70.

4.3 SFF with Different Right Ascension of the Ascending Node

So far, only near-polar satellite orbits are considered in our simulations. This kind of orbits causes resonance effects (Kvas et al. 2019), which together with drift of the EA in the low frequency domain, lead to the North-South striping behavior of the retrieved gravity field models. Hence, the North-South striping effect can be reduced either by utilizing the novel enhanced accelerometers or by providing additional measurements in the cross-track direction. One of the options for getting measurements in the cross-track direction could be by adding another satellite, see Fig. 6. In this section we consider two near-polar orbits ($i = 89°$) with the GRACE-like altitudes ($h = 450$ km) but with different RAAN angles $\Omega_1 = 127°$ and $\Omega_2 = 128°$. This brings a stable orbital configuration, i.e. the maximum distance at the equator between the satellites B and C does not increase over time, since the Ω does not impact the secular variations. In principle, this SFF could be treated as an enhanced version of the Pendulum constellation (Elsaka et al. 2014) with the difference that here, it is assumed that satellite C is always in cross-track direction w.r.t. the in-line along-track formation of the satellites A and B. The satellites A and B form an in-line GRACE-like formation separated by roughly $\rho = 200$ km. In this SFF, the two orbital planes intersect close
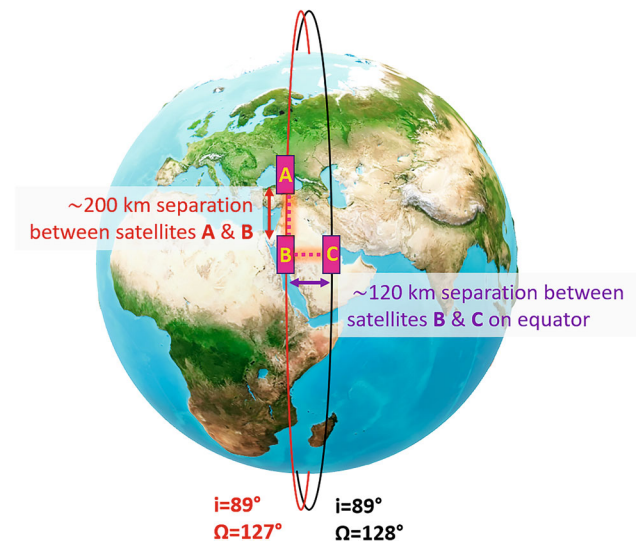
to the poles and the maximum separation between the orbits is at the equator, with about $l = 120$ km.

Different inter-satellite ranging instruments are assumed in the simulation of such a formation. For the in-line formation (satellites A and B) an anticipated LRI 2033 is assumed (blue curve in Fig. 2), while for the cross-track inter-satellite range measurement, a certain degradation of the laser beam steering mechanism due to increased tilt-to-length noise and the coupling caused by satellites pointing variations (Wegener et al. 2020) is considered. Furthermore, the current level of the pointing accuracies of the GRACE-like satellites, i.e. 2.5 rad in roll axis and 250 μrad in pitch and yaw (Goswami et al. 2021), is taken into account. Hence, a less accurate LRI 2023 (green curve on Fig. 2) is considered for the cross-track SFF.

However, on-board of all three satellites a SGRS Optical accelerometer derived in ACME was assumed (Kupriyanov et al. 2024). The same level of accuracy was taken for all three axes. Figure 7 shows the averaged error degree variance per specific degree in terms of geoid height for the in-line (blue curve), cross-track (orange curve) and combined formation (green curve). Identically to the previous graphs, the static gravity signal is depicted as a black dashed line. The in-line formation has a better performance than the cross-track formation. Combining these solutions at the level of normal equations (Wu 2016) with a weighting based on the posteriori variances results in the green curve.

Figure 8 represents global gravity field maps recovered from the in-line (top), cross-track (middle) and combined (bottom) satellite formations. Geoid height amplitudes represent the difference of the recovered gravity field models with the reference gravity field model EIGEN-6C4. The same order of magnitude of the spatial residuals, $\pm 5 \times 10^{-6}$ m, are used in all global maps for a more explicit difference. The combination of three satellites allow to get
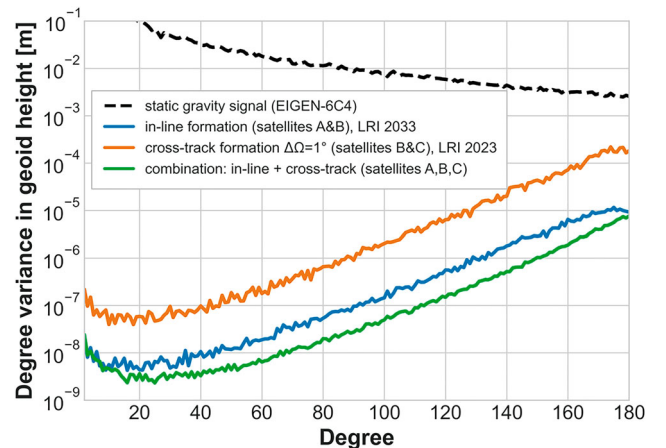

Fig. 6 Scheme of the combination of the in-line and cross-track formation differing by the right ascension of the ascending node (RAAN)

Fig. 7 Averaged error degree variance per specific degree in terms of geoid height of the in-line, cross-track and combined formations

Fig. 8 Global maps with the residuals in geoid heights, raw data, without post-processing and filtering. *Top*: In-line formation (satellites A and B); *Middle*: Cross-track formation (satellites B and C); *Bottom*: Combined formation (satellites A, B and C)
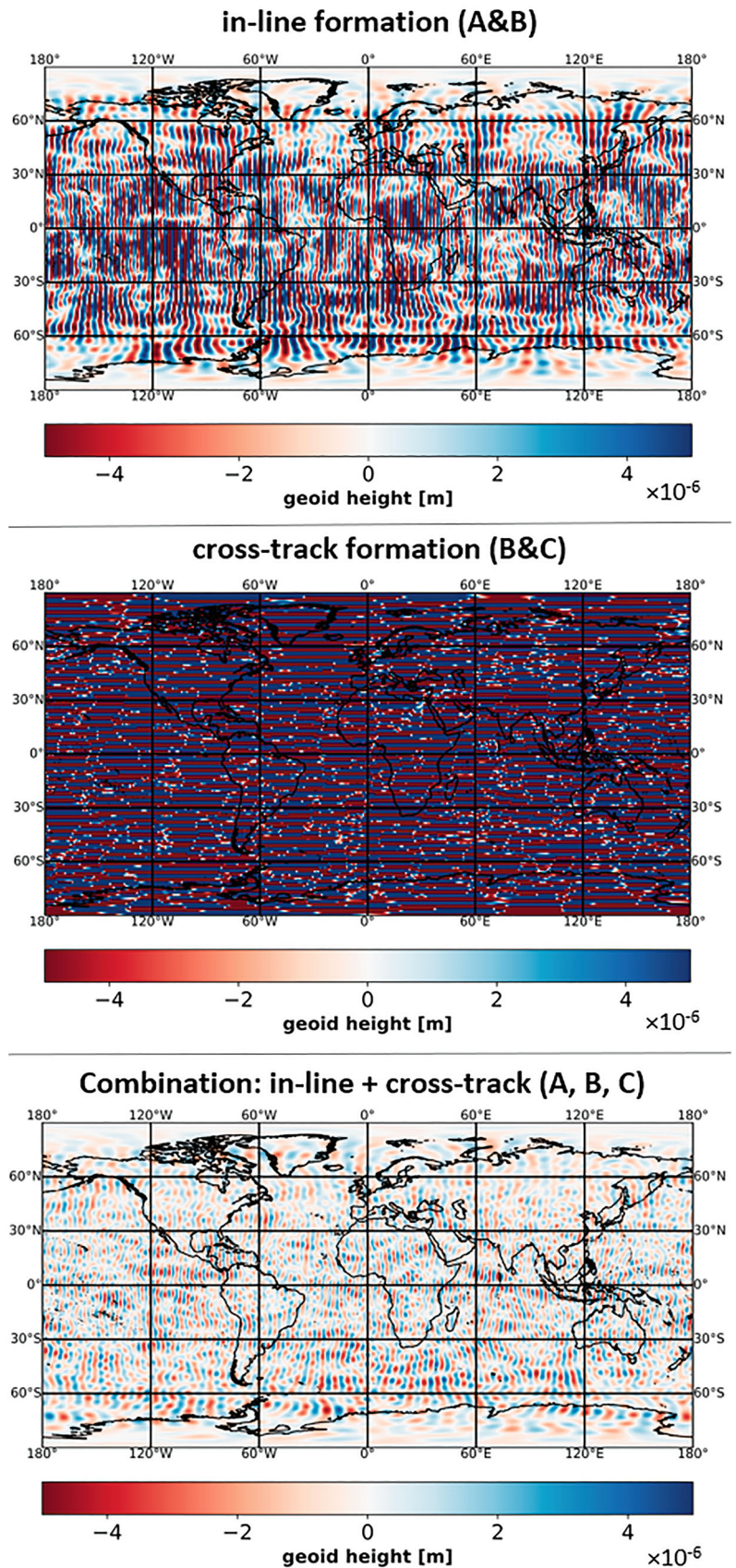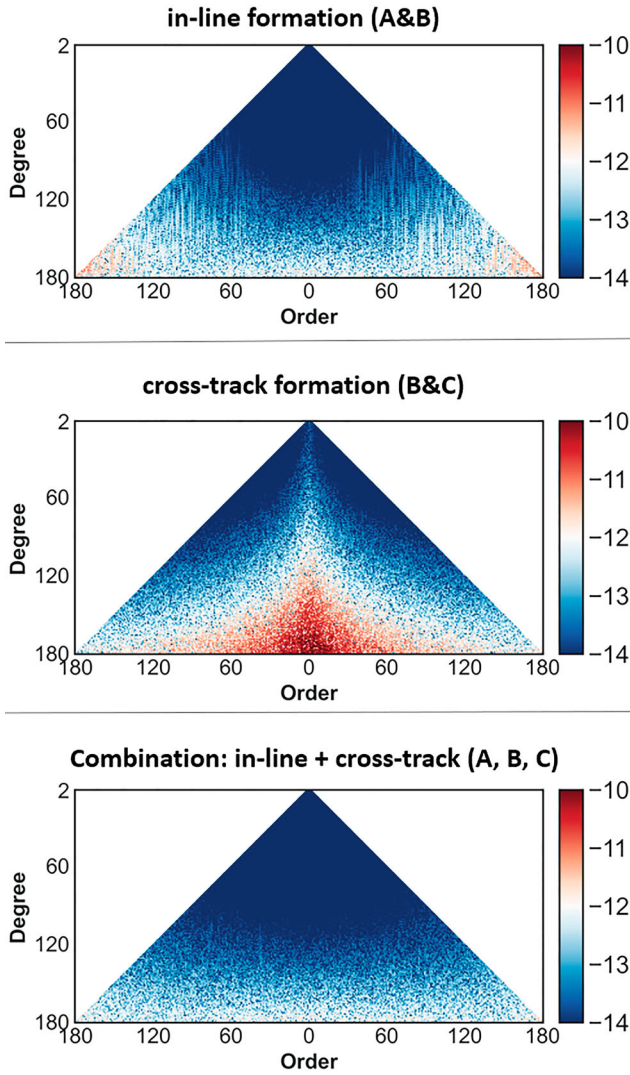
Fig. 9 Comparison of the spherical harmonic error spectra between in-line (top), cross-track (middle) and combined (bottom) formations

multi-directionality of the data by avoiding the North-South striping effect of the in-line formation without any post-processing or filtering.

Figure 9 shows the two dimensional spherical harmonic error spectrum or, in other words, the relative error of each spherical harmonic coefficient w.r.t. the reference gravity field. The color bars are given in logarithmic scale for better representation. On the top, we show the results from the in-line SFF, in the middle from the cross-track and at the bottom combined satellite formations.

It is worth mentioning that the cross-track range measurements in such SFF are technically challenging for current inter-satellite LRI systems due to the high (up to ± 130 m/s) relative range-rates between the satellites B and C. The current feasible range-rate for heterodyne lasers that were used on-board the GRACE-FO mission are ± 10 m/s (Sheard

et al. 2012; Elsaka et al. 2014), which is acceptable and sufficient even for the next upcoming missions to be launched in the time frame of 2028 to 2031 (Haagmans and Tsaoussi 2020; Massotti et al. 2021). However, in order to realize the additional cross-track link at some point, future developments should also focus extending the dynamic range of the LRI in terms of pointing angles and range rates.

4.4 SFF with Different Inclinations

Another satellite formation consisting of three satellites that could utilize information in the cross-track direction, is possible with orbits that differ by inclination, see Fig. 10. Similar to the previous SFF, this constellation assumed to have altitudes around 450 km, but inclinations equal to $i = 89.048°$ for the in-line and $i = 90.048°$ for the second orbital plane. However, a stable formation is not guaranteed (Elsaka 2012) in this case because of the secular perturbations of some Keplerian elements, in particular $\dot{\Omega}$ (Bloßfeld et al. 2014). It was found that after one month the maximum distance close to the poles in the cross-track direction between the satellites B and C increased from 120 to 520 km. In order to take into account adequately this increasing inter-satellite distance, an LRI 2023 model with $\rho = 600$ km baseline (yellow curve Fig. 2) was used for the cross-track formation.

After following the similar procedure as in the previous SFF, i.e. calculating the recovered gravity field from the in-line, cross-track and combined formations, the averaged error
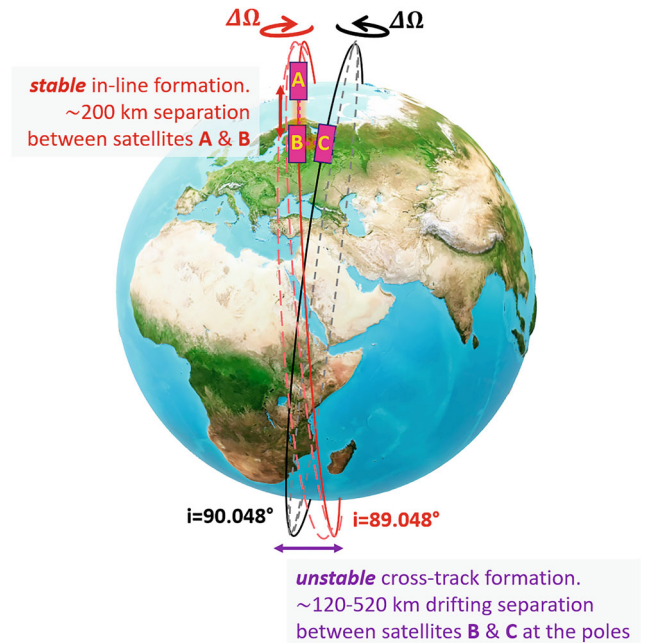

Fig. 10 Scheme of the combination of the in-line and cross-track formation differing by the inclination
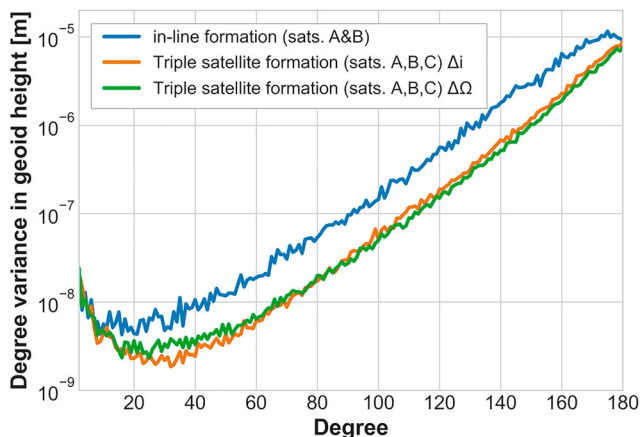
Fig. 11 Averaged error degree variance per specific degree in terms of geoid height of the in-line formation solely (blue), combined satellite formation with different RAAN (green) and combined satellite formation with different inclinations (orange)

degree variances per specific degree in terms of geoid height have been calculated. Figure 11 represents the comparison between the error degree variances from the in-line formation solely or, in other words, satellites A and B (blue curve), combined SFF from three satellites with different RAAN (green curve) and combined SFF with different inclinations (orange curve). In principle, combined solutions (green and orange curves) from both SFFs have a similar level of geoid accuracy. Up to degree 80, SFF with different inclinations show superior performance, while at higher degrees SFF with different RAAN performs better.

From technical point of view, SFF with different inclinations is even more technologically challenging than the one with different RAAN, because the relative range-rates between the satellites B and C are up to $\pm 600\,\text{m/s}$ here. This is 60 times larger than the current range-rate required for heterodyne lasers (Sheard et al. 2012; Elsaka et al. 2014). Furthermore, due to the unstable formation, a certain orbit maintenance has to be done in order to avoid drifting the orbital planes apart.

5 Conclusions

In this study, closed-loop simulations were performed in order to investigate the benefits of novel and enhanced instruments, i.e. accelerometers and gradiometers w.r.t. 'classical' electrostatic sensors. Moreover, static gravity field recovery from two novel triple satellite formations was carried out. To quantify the advantages of the novel instruments on the gravity field retrieval, the impact of temporal aliasing due to the insufficient background models was neglected.

Time-variable background models and associated aliasing errors are a major limiting factors in current satellite gravimetry. However, the background models will certainly be improved in future. It is anticipated that the processing strategies of gravitational data also enhance, for example, different parametrization, co-estimation of certain signals, etc. Therefore, one would be able to re-process data somewhen in future, as it was done with the GRACE or satellite altimetry data. There the observations from the 80s and 90s were re-processed benefiting from better orbits due to improved gravity field and reduction models. On the other hand, if sensors with poor performance are used in a mission, one can merely improve anything in post-processing. Therefore, it is necessary to consider the best possible sensors of a time on a mission and this study underlines what might be achieved in this respect. Moreover, the upcoming MAGIC mission, consisting of two satellite pairs, will also contribute to reducing the temporal aliasing effect (Purkhauser et al. 2020).

It was demonstrated that in low-low satellite-to-satellite configurations the static gravity field solutions could be improved up to three orders of magnitude with enhanced electrostatic, CAI and hybridized instruments

In single-axis cross-track gradiometry simulations, novel instruments also significantly improved the gravity field retrieval by one order of magnitude w.r.t. a GOCE-like electrostatic gradiometer. This would enable the geoid determination with a higher accuracy.

In addition, gravity field recovery results were investigated for two new satellite formation flights each with two orbital planes varying in RAAN or inclination relatively to each other. Both configurations showed an improvement in recovering the gravity field models from the combined solutions w.r.t. in-line and cross-track formations individually. However, the technical constraints, like formation maintenance with associated propellant consumption and maximum LRI range rates, make the option with RAAN separation more likely to be realized. Nonetheless, both alternative satellite formations would require significant modifications of the current GRACE-like platforms.

Further research is required to obtain more realistic simulations. This could be done in multiple ways, in particular with an improvement of the instrument modeling, e.g. analysing the noise budget of novel accelerometers, or including ancillary instruments in the gradiometry simulations, e.g. by providing additional angular velocity noise. Another to include time-variable gravity signals and related background models into the simulations. They are the source of the short-term mass variations from the atmosphere and oceans and produce aliasing errors which are typically the main contributors to inaccuracies in temporal gravity solutions.

2. European Union - CARIOQA-PMP (Project-ID 101081775)
3. German Aerospace Center (DLR) – Q-BAGS (Project-ID 50WM2181)
4. German Aerospace Center (DLR) – QUANTGRAV (Project-ID 50EE2220B)

References

Alonso I, Alpigiani C, Altschul B, et al (2022) Cold atoms in space: community workshop summary and proposed road-map. EPJ Quantum Technol 9(1):1–55. https://doi.org/10.1140/epjqt/s40507-022-00147-w

Armano M, Audley H, Baird J, et al (2018) Beyond the required LISA free-fall performance: New LISA pathfinder results down to 20 mHz. Phys Rev Lett 120(6):061101. https://doi.org/10.1103/PhysRevLett.120.061101

Armano M, Audley H, Baird J, et al (2021) Sensor noise in LISA pathfinder : In-flight performance of the optical test mass readout. Phys Rev Lett 126(13). https://doi.org/10.1103/PhysRevLett.126.131103

Barrett B, Cheiney P, Battelier B, Napolitano F, Bouyer P (2019) Multidimensional atom optics and interferometry. Phys Rev Lett 122(4):043604. https://doi.org/10.1103/PhysRevLett.122.043604

Bloßfeld M, Gerstl M, Hugentobler U, et al (2014) Systematic effects in LOD from SLR observations. Adv Space Res 54(6):1049–1063. https://doi.org/10.1016/j.asr.2014.06.009

Boulanger D, Christophe B, Rodrigues M, et al (2020) Future electrostatic accelerometer without polarization wire. European Geosciences Union General Assembly 2020, Online, 4–8 May 2020. https://doi.org/10.5194/egusphere-egu2020-4640

Chen J, Cazenave A, Dahle C, et al (2022) Applications and challenges of GRACE and GRACE Follow-On satellite gravimetry. Surv Geophys 43(1):305–345. https://doi.org/10.1007/s10712-021-09685-x

Christophe B, Boulanger D, Foulon B, et al (2015) A new generation of ultra-sensitive electrostatic accelerometers for GRACE Follow-on and towards the next generation gravity missions. Acta Astronautica 117:1–7. https://doi.org/10.1016/j.actaastro.2015.06.021

Dalin M, Christophe B, Liorzou F, et al (2020) ONERA accelerometers for future gravity mission. European Geosciences Union General Assembly 2020, online poster

Daras I, Pail R (2017) Treatment of temporal aliasing effects in the context of Next Generation satellite Gravimetry Missions. J Geophys Res Solid Earth 122(9):7343–7362. https://doi.org/10.1002/2017JB014250

Dávila Álvarez A, Knudtson A, Patel U, et al (2022) A simplified gravitational reference sensor for satellite geodesy. J Geodesy 96(10):70. https://doi.org/10.1007/s00190-022-01659-0

Dobslaw H, Bergmann-Wolf I, Dill R, et al (2015) The updated ESA Earth System Model for future gravity mission simulation studies. J Geodesy 89:505–513. https://doi.org/10.1007/s00190-014-0787-8

Elsaka B (2012) Simulated satellite formation flights for detecting the temporal variations of the earth's gravity field. PhD thesis, Rheinische Friedrich-Wilhelms-Universität Bonn. https://hdl.handle.net/20.500.11811/4203

Elsaka B, Raimondo J-C, Brieden P, et al (2014) Comparing seven candidate mission configurations for temporal gravity field retrieval through full-scale numerical simulation. J Geodesy 88:31–43. https://doi.org/10.1007/s00190-013-0665-9

Flechtner F, Reigber C, Rummel R, et al (2021) Satellite gravimetry: A review of its realization. Surv Geophys 42(5):1029–1074. https://doi.org/10.1007/s10712-021-09658-0

Förste C, Bruinsma S, Flechtner F, et al (2011) EIGEN-6C3 - The latest Combined Global Gravity Field Model including GOCE data up to degree and order 1949 of GFZ Potsdam and GRGS Toulouse. In: AGU Fall Meeting Abstracts, vol 2011, pp G51A–0860. Harvard ASD: 2011AGUFM.G51A0860F

Frommknecht B, Oberndorfer H, Flechtner F, et al (2003) Integrated sensor analysis for GRACE–development and validation. Adv Geosci 1:57–63

Frommknecht B, Fackler U, Flury J (2006) Integrated sensor analysis GRACE. In: Flury J, et al (eds), Observation of the Earth system from space. Springer, pp 99–113. doi: 10.1007/3-540-29522-4_8

Goswami S, Francis SP, Bandikova T, et al (2021) Analysis of GRACE Follow-On Laser Ranging Interferometer derived inter-satellite pointing angles. IEEE Sensors J, 1. https://doi.org/10.1109/JSEN.2021.3090790

Haagmans R, Tsaoussi L (2020) Next generation gravity mission as a Mass-change And Geosciences International Constellation (MAGIC) mission requirements document. Earth and Mission Science Division, European Space Agency; NASA Earth Science Division. https://doi.org/10.5270/esa.nasa.magic-mrd.2020

HosseiniArani A, Tennstedt B, Schilling M, et al (2022) Kalman-filter based hybridization of classic and cold atom interferometry accelerometers for future satellite gravity missions. In: International Association of Geodesy Symposia. https://doi.org/10.1007/1345_2022_172

HosseiniArani A, Schiling M, Beaufils Q, et al (2024) Advances in atom interferometry and their impacts on the performance of quantum accelerometers on-board future satellite gravity missions. Adv Space Res. https://doi.org/10.1016/j.asr.2024.06.055

Knabe A, Schilling M, Wu H, et al (2022) The benefit of accelerometers based on cold atom interferometry for future satellite gravity missions. International Association of Geodesy Symposia. Springer, Berlin, Heidelberg. https://doi.org/10.1007/1345_2022_151

Kupriyanov A, Reis A, Schilling M, et al (2024) Benefit of enhanced electrostatic and optical accelerometry for future gravimetry missions. Adv Space Res, 73. https://doi.org/10.1016/j.asr.2023.12.067

Kvas A, Behzadpour S, Ellmer M, et al (2019) ITSG–Grace2018: overview and evaluation of a new GRACE–only gravity field time series. J Geophys Res Solid Earth 124(8):9332–9344. https://doi.org/10.1029/2019JB017415

Lévèque T, Fallet C, Lefebve J, et al (2023) CARIOQA: Definition of a quantum pathfinder mission. In: International Conference on Space Optics–ICSO 2022, vol 12777, pp 1536–1545. SPIE. arXiv:2211.01215

Liorzou F, Lebat V, Christophe B, et al (2023) ONERA accelerometers for future gravity mission. In: EGU General Assembly, Vienna, Austria. https://doi.org/10.5194/egusphere-egu23-8155

Marque J-P, Christophe B, Foulon B (2010) Accelerometers of the GOCE mission: return of experience from one year of in-orbit. In: Proceedings of the ESA Living Planet Symposium, Bergen, Norway. Harvard ADS: 2010ESASP.686E..57M

Massotti L, Siemes C, March G, et al (2021) Next generation gravity mission elements of the mass change and geoscience international constellation: from orbit selection to instrument and mission design. Remote Sensing 13(19):3935. https://doi.org/10.3390/rs13193935

Mehta PM, Walker AC, Sutton EK, et al (2017) New density estimates derived using accelerometers on board the CHAMP and GRACE satellites. Space Weather 15(4):558–576

Pail R, Bingham R, Braitenberg C, et al (2015) Science and user needs for observing global mass transport to understand global change and to benefit society. Surv Geophys 36(6):743–772. https://doi.org/10.1007/s10712-015-9348-9

Pail R, Bamber J, Biancale R, et al (2019) Mass variation observing system by high low inter-satellite links (MOBILE)—a new concept for sustained observation of mass transport from space. J Geodetic Sci 9(1):48–58. https://doi.org/10.1515/jogs-2019-0006

Panet I, Narteau C, Lemoine J-M, et al (2022) Detecting preseismic signals in GRACE gravity solutions: Application to the 2011 Tohoku

M w 9.0 earthquake. J Geophys Res Solid Earth 127(8). https://doi.org/10.1029/2022JB024542

Peidou A, Landerer F, Wiese D, et al (2022) Spatiotemporal characterization of geophysical signal detection capabilities of GRACE–FO. Geophys Res Lett 49(1). https://doi.org/10.1029/2021GL095157

Purkhauser AF, Siemes C, Pail R (2020) Consistent quantification of the impact of key mission design parameters on the performance of next-generation gravity missions. Geophysl J Int 221(2):1190–1210. https://doi.org/10.1093/gji/ggaa070

Savoie D, Altorio M, Fang B, et al (2018) Interleaved atom interferometry for high-sensitivity inertial measurements. Sci Adv 4(12):eaau7948. https://doi.org/10.1126/sciadv.aau7948

Sheard B, Heinzel G, Danzmann K, et al (2012) Intersatellite laser ranging instrument for the GRACE follow-on mission. J Geodesy 86:1083–1095. https://doi.org/10.1007/s00190-012-0566-3

SILSO World Data Center (2023) International Sunspot Number Monthly Bulletin and online catalogue. http://www.sidc.be/silso/

Sumner TJ, Mueller G, Conklin JW, et al (2020) Charge induced acceleration noise in the LISA gravitational reference sensor. Classical Quantum Gravity 37(4):045010. https://doi.org/10.1088/1361-6382/ab5f6e

Torge W, Müller J, Pail R (2023) Geodesy. de Gruyter. ISBN 3110723301

Touboul P, Metris S, Le Traon O, et al (2016) Gravitation and geodesy with inertial sensors, from ground to space. AerospaceLab 12. https://doi.org/10.12762/2016.AL12-11

Trimeche A, Battelier B, Becker D, et al (2019) Concept study and preliminary design of a cold atom interferometer for space gravity gradiometry. Classical Quantum Gravity 36(21):215004. https://doi.org/10.1088/1361-6382/ab4548

van Camp M, Pereira dos Santos F, Murböck M, et al (2021) Lasers and ultracold atoms for a changing Earth. Eos Trans Am Geophys Union 102. https://doi.org/10.1029/2021EO210673f

Weber WJ, Bortoluzzi D, Bosetti P, et al (2022) Application of LISA gravitational reference sensor hardware to future intersatellite geodesy missions. Remote Sensing 14(13):3092. https://doi.org/10.3390/rs14133092

Wegener H, Müller V, Heinzel G, et al (2020) Tilt-to-length coupling in the GRACE Follow-On laser ranging interferometer. 0022-4650, pp 1–10. https://doi.org/10.2514/1.A34790

Wöske F, Kato T, List M, et al (2016) Development of a high precision simulation tool for gravity recovery missions like GRACE. In: Proceedings of the 26th AAS/AIAA Space Flight Mechanics Meeting, 14.-18.02.2016, Napa, Califonia, USA, pp 14–18

Wöske F, Kato T, Rievers B, et al (2018) GRACE accelerometer calibration by high precision non-gravitational force modeling. Adv Space Res 63(3):1318–1335. https://doi.org/10.1016/j.asr.2018.10.025

Wu H (2016) Gravity field recovery from GOCE observations. PhD thesis, Fakultät für Bauingenieurwesen und Geodäsie - Leibniz Universität Hannover

Xiao Y, Yang Y, Pan Z, et al (2023) Performance and application of the Chinese satellite-to-satellite tracking gravimetry system. Chinese Sci Bull 68:2655–2664. https://doi.org/10.1360/TB-2022-1057

Zahzam N, Christophe B, Lebat V, et al (2022) Hybrid electrostatic–atomic accelerometer for future space gravity missions. Remote Sensing 14(14):3273. https://doi.org/10.3390/rs14143273